Dislocation geometry in the TGB_A phase: Linear theory

Igor Bluestein, Randall D. Kamien, and T. C. Lubensky
Department of Physics and Astronomy, University of Pennsylvania, Philadelphia, Pennsylvania 19104
(Received 17 January 2001; published 14 May 2001)

We demonstrate that an arbitrary system of screw dislocations in a smectic-*A* liquid crystal may be consistently treated within harmonic elasticity theory, provided that the angles between dislocations are sufficiently small. Using this theory, we calculate the ground-state configuration of the TGB_A phase. We obtain an estimate of the twist-grain-boundary spacing and screw dislocation spacing in a boundary in terms of the macroscopic parameters, in reasonable agreement with experimental results.

DOI: 10.1103/PhysRevE.63.061702 PACS number(s): 61.30.Jf, 61.30.Cz, 61.72.Ji, 61.72.Mm

I. INTRODUCTION

Condensed matter systems offer a vast stage for the intricate interplay between order and disorder. A beautiful example of such interplay is the twist-grain-boundary phase (TGB) of chiral smectics, which is the liquid-crystalline analog of the Abrikosov vortex state of type II superconductors [1,2]. Morphologically, the phase consists of blocks of pure smectic (which can be either smectic-*A* or smectic-*C*) separated by parallel, regularly spaced twist grain boundaries, where each boundary is formed by a periodic array of screw dislocations. The direction of dislocation lines rotates by a constant angle from one grain boundary to the next. Such a dislocation arrangement causes the smectic blocks to rotate about the axis perpendicular to the grain boundaries dragging the nematic director along. Thus the TGB structure combines the properties of smectics and cholesterics: the nematic director twists on average as in cholesterics while the lamellar structure of a smectic is preserved. In this paper only the TGB_A phase will be considered. As suggested by its name, the smectic blocks in TGB_A are smectic-*A*.

The analogy between the TGB_A phase and the Abrikosov vortex lattice is based on the mathematical similarity of the Gibbs free energies for metals in a magnetic field and for chiral smectics [1–4]. Their respective forms, known as the Ginzburg-Landau free energy and the de Gennes free energy, are

$$G_{\mathrm{GL}}=\int d^3x\left[\frac{1}{2m^*}\left|\left(\frac{\hbar}{i}\nabla-\frac{e^*}{c}\mathbf{A}\right)\psi\right|^2+r|\psi|^2+\frac{1}{2}g|\psi|^4+\frac{1}{8\pi\mu}(\nabla\times\mathbf{A})^2-\frac{\mathbf{H}}{4\pi}\cdot\nabla\times\mathbf{A}\right], \tag{1.1}$$

and

$$\begin{aligned}G_{\mathrm{deG}}=\int d^3x[&C_\perp(\nabla-iq_0\mathbf{n})\psi(\nabla+iq_0\mathbf{n})\psi^*\\&+(C_\parallel-C_\perp)n_in_j(\nabla-iq_0\mathbf{n})_i\psi(\nabla+iq_0\mathbf{n})_j\psi^*\\&+r|\psi|^2+\tfrac{1}{2}g|\psi|^4+\tfrac{1}{2}K_1(\nabla\cdot\mathbf{n})^2+\tfrac{1}{2}K_2(\mathbf{n}\cdot\nabla\times\mathbf{n})^2\\&+\tfrac{1}{2}K_3[\mathbf{n}\times(\nabla\times\mathbf{n})]^2-h\mathbf{n}\cdot(\nabla\times\mathbf{n})],\end{aligned} \tag{1.2}$$

where ψ is a complex order parameter, $\mathbf{A}$ the vector potential, $\mathbf{H}$ the magnetic intensity, h a chiral field determined by molecular structure [5], and $\mathbf{n}$ the unit director, often decomposed as $\mathbf{n}=\mathbf{n}_0+\delta\mathbf{n}$. The Ginzburg-Landau free energy (1.1) defines two characteristic length scales: the order parameter coherence length $\xi=(\hbar^2/2m^*|r|)^{1/2}$ and the magnetic field penetration depth $\lambda=(m^*c^2g/4\pi\mu e^{*2}|r|)^{1/2}$. Their ratio $\kappa=\lambda/\xi$, called the Ginzburg parameter, controls the phase diagram as a function of temperature and external magnetic field. When the Ginzburg parameter is less than the critical value $\kappa_c=1/\sqrt{2}$, the system is type I, and there is a first-order transition between a normal metal in a field and the Meissner phase with $\psi=\mathrm{const}\neq 0$ and magnetic field $\mathbf{B}=0$. When $\kappa>\kappa_c$, the system becomes type II, and a new phase intervenes between the normal-metal state and the Meissner state. This new phase, the Abrikosov flux phase, is characterized by a proliferation of linear topological defects of the complex order parameter field ψ. The defects are magnetic flux lines, and they form a two-dimensional triangular lattice throughout the phase.

A very similar phenomenon occurs in chiral smectics, only the situation becomes somewhat more complicated because of anisotropy of the de Gennes free energy (we note that the theory of anisotropic superconductors is equally complex, see, e.g., [6]). Instead of a single order parameter coherence length ξ, there are two lengths: the transverse coherence length $\xi_\perp=(C_\perp/|r|)^{1/2}$ and the longitudinal coherence length $\xi_\parallel=(C_\parallel/|r|)^{1/2}$. But since the values of $C_\perp$ and $C_\parallel$ can be made equal by rescaling of coordinates, we will not be concerned with making distinctions between $\xi_\perp$ and $\xi_\parallel$ and assume $\xi_\perp\approx\xi_\parallel\approx\xi$. The chiral smectic analog of the magnetic field penetration depth is the twist penetration depth $\lambda_2=(K_2g/2Cq_0^2|r|)^{1/2}$, where $C\approx C_\perp\approx C_\parallel$. As in superconductors, the chiral Ginzburg parameter $\kappa_2=\lambda_2/\xi$ in liquid crystals determines the structure of the phase diagram as a function of temperature and chiral coupling h. Again, a defect phase, which is now the TGB_A phase, appears on the phase diagram when $\kappa_2>1/\sqrt{2}$. Linear topological defects in the TGB_A phase are screw dislocations arranged in twist grain boundaries.

An important problem in the theory of the defect phases predicted by the Gibbs free energies (1.1) and (1.2) is to relate the lattice parameters of defect lattices to the coupling strengths that enter these energies. This is rather complicated

because the Gibbs energies (1.1) and (1.2) include fouth-order terms that lead to nonlinear Euler-Lagrange equations. Nevetheless, since the publication of Abrikosov's paper over 44 years ago [7], an extensive body of both experimental and theoretical work on the vortex arrangement in the Abrikosov phase has been performed, covering all possible ranges of the external magnetic field, temperature, and Ginzburg parameter [8,9]. In contrast with this happy situation in superconductors, there is only a small literature that address the liquid-crystal version of the problem, namely, the determination of the grain-boundary spacing l_b and the dislocation spacing l_d within a grain boundary. In part this is due to the fact that rotation of defects in TGB_A makes this version of the problem more complicated.

In their original paper [1] Renn and Lubensky considered the TGB_A lattice structure near the upper critical field h_{c2} marking the transition from the cholesteric to the TGB phase. They employed a model free energy with $C_\perp = C_\parallel$ and $K_1 = K_3 \equiv K$. Additionally, they assumed that the twist pitch is very large in comparison to a smectic layer spacing. Under these assumptions, in a calculation that parallels Abrikosov's calculation [7], they computed the ratio l_b/l_d for $\kappa_2 = 0.80 > 1/\sqrt{2}$ and various values of K/K_2. They found that l_b/l_d increases from 0.95 for $K/K_2 = 0$ to 1.45 for $K/K_2 = 10^4$. In other words, l_b/l_d is *sensitive* to the relative values of the Frank elastic constants. Our approach, which applies near H_{c1}, is applicable when the rotation angle between consecutive smectic blocks is small, predicts a value close to 0.95 for *all* values of K/K_2.

Experimental determination of the TGB_A lattice parameters has proven to be a difficult task. Early experiments [10–13] were crucial in establishing the existence of the defect phase of chiral smectics and confirmed that the morphology of this phase agrees with the predictions of Renn and Lubensky. However, in all these experiments l_b and l_d were estimated rather than measured. Recently an extensive structural study of the TGB_A phase occurring in a series of chiral tolane derivatives [14] was undertaken by Navailles and co-workers [15]. They observed an x-ray diffraction pattern in the transverse direction to the pitch axis that consisted of discrete Bragg spots, which provided a direct way to measure the rotation angle $\Delta\Theta$ of smectic blocks. Since the smectic layer spacing d is easy to measure in the same experiment, it has now become possible to obtain the precise values of l_d via $d/2l_d = \sin(\Delta\Theta/2)$. As an additional benefit, the information regarding the number of smectic blocks per pitch provided a way to compute the block size from the pitch values measured in a different set of experiments based on the observation of the Grandjean-Cano steps [16]. The ratio l_b/l_d was found to vary from 0.74 to 1.08. Whereas the exact value l_b/l_d is up to interpretation, these experiments are a clear indication that this ratio remains close to 1.

In this paper the equilibrium dislocation arrangement in the TGB_A phase is considered in the limit of low-angle grain boundaries. Formally, this limit is appropriate close to the lower critical field h_{c1}, marking the transition from the smectic-*A* phase to the TGB_A phase. In this case the dislocation density is low, and it is possible to neglect the interaction between dislocation cores, so the dislocation core energy associated with destruction of the order parameter produces an extensive term in the total free energy. Thus, in this case, the lattice structure is determined completely by the elastic energy cost of the distorted smectic structure induced by the presence of screw dislocations. In the language of superconductivity, this is the London limit of the Ginzburg-Landau equations. For our analysis, this means that the results for the structure of a single vortex and the systems of parallel vortices obtained in the theory of superconductors may be directly translated to the language of liquid crystals using the Gibbs energies (1.1) and (1.2) as a dictionary. We will show that there is a simple way to generalize the results for parallel dislocations to the case of interacting twist grain boundaries. In the low-angle limit, the rotation angle is a natural small paramater, and to the lowest order in this parameter, the interaction energy of two twist grain boundaries composed of *discrete* linear defects turns out to be the same as that of grain boundaries with *continuous* defect distribution. This observation allows us to compute the energy cost for the dislocation arrangement in the TGB_A phase analytically.

The paper is organized as follows. Section II introduces the elastic fields suitable for type II smectics-*A*. We construct the elastic free energy functional in the harmonic approximation. We demonstrate that if we have a solution for the elastic fields uniform in the direction of the layer normal at infinity, it is possible to construct more general solutions by superimposing shifted and rotated copies of the original solution. In Sec. III we show that in the harmonic approximation, systems of pure screw dislocations in smectics are distinguished from other dislocation systems by a constraint that sets the smectic layers to be minimal surfaces. We compute the distortion fields and the elastic energy of systems of parallel screw dislocations. In Sec. IV we calculate the elastic energy of an individual twist grain boundary and the interaction energy of two twist grain boundaries. In Sec. V we obtain the elastic energy density for the TGB_A phase. Adding two extensive terms to it, we construct the total free energy density. Its minimization yields preferred values for the grain boundary spacing and the dislocation spacing within a grain boundary for the given values of material parameters. We find that in the low-angle regime the ratio l_d/l_b is practically constant over a wide range of the control parameters, and its value is 0.95.

II. SUPERPOSITION OF SOLUTIONS FOR DISTORTION FIELDS

The elastic free energy for smectics-*A* directly follows from the de Gennes free energy (1.2) by assuming $|\psi|^2$ to be fixed. Because the smectic density is rapidly varying, it is standard to write down the elastic free energy of smectics in terms of the layer displacement field u related to the phase Φ of the order parameter $\psi = e^{i\Phi}$ by a decomposition

$$\phi \equiv \Phi/q_0 = \mathbf{n}_0 \cdot \mathbf{x} - u(\mathbf{x}), \tag{2.1}$$

where $\mathbf{n}_0$ is a fixed unit vector. It is important to note that in principle $\mathbf{n}_0$ can be chosen to point in an arbitrary direction

and the elastic free energy must be invariant under rotations of $\mathbf{n}_0$. In some sense, picking $\mathbf{n}_0$ is like fixing a gauge. Dropping the constant terms, choosing $\mathbf{n}_0$ to be in the $\hat{z}$ direction, and denoting $\mathbf{n}-\mathbf{n}_0$ as $\delta\mathbf{n}$, $2q_0^2|\psi|^2C_\parallel$ as B, $2q_0^2|\psi|^2C_\perp$ as D, we have, to quadratic order in $\delta\mathbf{n}$

$$F=\tfrac{1}{2}\int d^3x[B(\partial_z u)^2+D(\boldsymbol{\nabla}_\perp u-\delta\mathbf{n})^2+K_1(\boldsymbol{\nabla}_\perp\cdot\delta\mathbf{n})^2 +K_2(\boldsymbol{\nabla}_\perp\times\delta\mathbf{n})^2+K_3(\partial_z\delta\mathbf{n})^2]. \tag{2.2}$$

This form of the smectic elastic free energy is known as the harmonic approximation. Note that the de Gennes free energy and, consequently, the elastic free energy (2.2) derived from it are invariant with respect to small rotations but not with respect to arbitrary rotations. Therefore, their validity is limited to only those smectic configurations where the smectic layer normal $\mathbf{N}$ and the nematic director $\mathbf{n}$ do not deviate significantly from $\mathbf{n}_0$.

The Euler-Lagrange equations derived from the free energy (2.2) are linear, so it is easy to construct new solutions by superimposing the ones already known. To do this, we will exploit an underlying symmetry of the full theory (1.2). Under an arbitrary rotation $\mathbf{R}$, ϕ, and $\mathbf{n}$ transform as

$$\phi'(\mathbf{x})=\phi(\mathbf{R}\mathbf{x}), \tag{2.3}$$

$$\mathbf{n}'(\mathbf{x})=\mathbf{R}^{-1}\mathbf{n}(\mathbf{R}\mathbf{x}). \tag{2.4}$$

The displacement field u' inherits its transformation properties through its definition $u\equiv\mathbf{n}_0\cdot\mathbf{x}-\phi$. In general this transformation is nonlinear in the rotation angle θ. However, since we are interested in small rotations, we may expand the transformation laws (2.3) and (2.4) in the rotation angle θ and keep only the linear terms.

Consider the distortion fields u and $\delta\mathbf{n}$ produced by a linear source perpendicular to undistorted smectic layers at infinity. We will construct rotated solutions by modifying simpler solutions: without loss of generality, we initially take our source to point along the $\hat{z}$-axis. If we choose $\mathbf{n}_0=\hat{z}$, the distortion fields will be independent of z:

$$\phi(x,y,z)=z-u(x,y), \tag{2.5}$$

$$\delta\mathbf{n}(x,y,z)=\delta\mathbf{n}(x,y). \tag{2.6}$$

We may construct a solution that corresponds to a superposition of sources that intersect the xy plane at (x^α,y^α) and oriented along $\mathbf{N}_0^\alpha=\hat{z}+\theta^\alpha\mathbf{t}^\alpha$, where $\mathbf{t}^\alpha$ is a unit vector orthogonal to $\hat{z}$ and $\theta^\alpha\ll 1$. First, consider what happens to the original solution if the system undergoes a rigid physical rotation about x axis by a small angle θ. The phase function ϕ is a scalar, so the transformed function is just the original function of the transformed coordinates:

$$\phi'(x,y,z)=\phi(x',y',z')=\phi(x,y-\theta z,z+\theta y). \tag{2.7}$$

In terms of the original elastic field u, the transformed phase function is

$$\phi'(x,y,z)=z+\theta y-u(x,y-\theta z). \tag{2.8}$$

We can read the decomposition (2.8) in two ways. In the first version, it defines the rotated elastic field $u'(x,y,z)$ with respect to $\mathbf{n}_0'=\hat{z}+\theta\hat{y}$:

$$u'(x,y,z)=u(x,y-\theta z). \tag{2.9}$$

The corresponding transformation of $\delta\mathbf{n}$ is

$$\delta\mathbf{n}'(x,y,z)=\delta\mathbf{n}(x,y-\theta z). \tag{2.10}$$

If we consider the effect of rotations in Fourier space, we note that if

$$g(x,y,z)=\int\frac{d^3q}{(2\pi)^3}g(q_x,q_y,q_z)e^{iq_xx}e^{iq_yy}e^{iq_zz}, \tag{2.11}$$

then it follows that

$$g'(q_x,q_y,q_z)\approx g(q_x,q_y-\theta q_z,q_z+\theta q_y). \tag{2.12}$$

The second interpretation of Eq. (2.8) is as a definition of the rotated field u'' with respect to the original $\mathbf{n}_0=\hat{z}$. In this case, the transformed elastic fields acquire an extra asymptotic term, linear in y:

$$u''(x,y,z)=-\theta y+u(x,y-\theta z), \tag{2.13}$$

$$\delta\mathbf{n}''(x,y,z)=\theta\hat{y}+\delta\mathbf{n}(x,y-\theta z). \tag{2.14}$$

Even if we have a superposition of sources of different orientation, the elastic fields u_α'', $\delta\mathbf{n}_\alpha''$ produced by individual sources are all defined with respect to the same fiducial choice of $\mathbf{n}_0=\hat{z}$, so it is consistent to superimpose these fields and claim that this superposition of fields is the solution for the superposition of sources:

$$u_{\text{super}}(x,y,z)=\sum_\alpha\ [-\theta^\alpha\mathbf{t}^\alpha\cdot\mathbf{x}+u(\mathbf{x}_\perp-\mathbf{x}_\perp^\alpha-\theta^\alpha\mathbf{t}^\alpha z)], \tag{2.15}$$

$$\delta\mathbf{n}_{\text{super}}(x,y,z)=\sum_\alpha\ [\theta^\alpha\mathbf{t}^\alpha+\delta\mathbf{n}(\mathbf{x}_\perp-\mathbf{x}_\perp^\alpha-\theta^\alpha\mathbf{t}^\alpha z)]. \tag{2.16}$$

where u_{super} and $\delta\mathbf{n}_{\text{super}}$ are the total displacement and director fields, respectively. The asymptotic parts of the distortion fields are absolutely essential in formulating global geometric constraints on smectic configurations, in particular, for distinguishing different types of dislocations. When constructing linear superpositions of defects we must make sure that the layer normals are unambiguously defined everywhere. Fortunately, the terms linear in y drop out of the energetics. As a result we are free to use either $u'(x,y,z)$ or $u''(x,y,z)$ in our calculations. We will exploit this fact in the next section.

III. INTERACTION ENERGY OF SCREW DISLOCATIONS

A. Screw dislocations vs edge dislocations

Dislocations in smectics are linear topological defects of the lamellar structure [2,17]. In the presence of dislocations, it becomes impossible to devise a consistent global numbering scheme for the smectic layers. In other words, the phase field Φ cannot be defined as a continuous field for the whole region where the smectic order parameter is defined. If a closed contour surrounds a dislocation core and one insists that Φ be continuous, then the phase differences along the contour will add up to a multiple of 2π:

$$\oint d\Phi = 2\pi n. \tag{3.1}$$

However, it is possible to break the space into a number of overlapping regions and define Φ for each region in such a way that local definitions of Φ differ in the intersections of regions only by a constant. In this case the gradient field $\nabla\Phi$ is globally defined (single-valued and continuous). If we choose the same ''gauge'' $\mathbf{n}_0$ for each region, then the field $\mathbf{v} \equiv -\nabla_\perp u$ defined by $\nabla\phi \equiv \nabla(\Phi/q_0) = \mathbf{n}_0 + \mathbf{v}$ will be also globally consistent. In terms of $\mathbf{v}$, the above integral can be rewritten as

$$\oint \mathbf{v}\cdot d\mathbf{l} = nd. \tag{3.2}$$

It is convenient to represent a dislocation line of strength n and position $\mathbf{x}=\mathbf{x}(l)$ by a singular dislocation density

$$\mathbf{b}(\mathbf{x}) = d\int dl \frac{d\mathbf{x}(l)}{dl} n\,\delta^{(3)}(\mathbf{x}-\mathbf{x}(l)). \tag{3.3}$$

With its help, the integral relation (3.2) can be turned into a differential form:

$$\nabla\times\mathbf{v} = \mathbf{b}(\mathbf{x}). \tag{3.4}$$

For a system of dislocations, the density is constructed by superimposing densities of individual lines in the form (3.3). Clearly, this procedure guarantees that all integrals in the form (3.1) or (3.2) will have the right value. In the most general case, distributions of dislocations can be continuous. In principle, any function $\mathbf{b}(\mathbf{x})$ can be considered to be a dislocation density as long as it satisfies a conservation law $\nabla\cdot\mathbf{b}=0$, which says that dislocation lines cannot end inside the system.

The integral constraints (3.1) and (3.2) or their differential equivalent (3.4), define dislocations topologically, but by their nature they are incapable of determining how dislocations are actually arranged in physical systems. To understand that, we need to look at dislocations as physical objects that have energy. There are two contributions to the dislocation energy. The core energy $F_{\rm core}$ arises from the destruction of the order parameter in the core region. It is proportional to the total length of dislocation lines in the system, but does not depend on the details of the smectic configuration outside the core. Still, for topological reasons, the smectic structure outside the core is necessarily distorted, and these distortions give rise to the elastic energy $F_{\rm el}$ of the dislocation.

The structure of the distortion fields induced by a dislocation depends significantly on the orientation of the dislocation core with respect to the smectic layers. This orientation reflects the physical nature of the dislocation. We may consider the Volterra construction for two classes of defects [2]. One way to produce a dislocation in a smectic is to force the layers to wind in a helical fashion, which causes the core to be perpendicular to the smectic layers at infinity. A physically different procedure is to remove half a layer, which makes the core parallel to the layers. Dislocations of the first type are known as screw dislocations and of the second type as edge dislocations.

Now let us turn to calculation of the elastic energy of a system of screw dislocations. The program is to construct an appropriate dislocation density $\mathbf{b}(\mathbf{x})$ and then minimize the smectic elastic free energy while requiring compliance with Eq. (3.4). If we restrict our consideration to systems of nearly parallel screw dislocations with separations large compared to the preferred layer spacing d, then the criteria for the validity of the harmonic approximation are met and we can use the elastic free energy (2.2).

First, consider a single screw dislocation at the origin. The corresponding dislocation density is

$$\mathbf{b}_1(\mathbf{x}) = \hat{z}\,d\,\delta(x)\,\delta(y). \tag{3.5}$$

If we make the natural choice $\mathbf{n}_0=\hat{z}$, the distortion fields $\mathbf{v}$ and $\delta\mathbf{n}$ are cylindrically symmetric. It turns out that the cylindrical symmetry and the topological condition (3.4) completely determine the $\mathbf{v}$-field.

An immediate consequence of the cylindrical symmetry of $\mathbf{v}$ and $\delta\mathbf{n}$ is that their derivatives in the z direction vanish: $\partial_z\mathbf{v}=0$, $\partial_z\delta\mathbf{n}=0$. The x and y components of the topological condition (3.4), imply that $\partial_y v_z=0$ and $\partial_x v_z=0$. It then follows that v_z is constant, set to zero by the boundary conditions at infinity:

$$v_z = 0. \tag{3.6}$$

Therefore, the layer displacement field u is independent of z, and the distortion fields induced by a single screw dislocation are of the type considered in the previous section. Thus, we may construct the distortion fields for the entire system of nearly parallel screw dislocations by the superposition procedure of Eqs. (2.15) and (2.16).

There is another constraint on the distortion fields imposed by the cylindrical symmetry. Since $\partial_z\mathbf{v}$ and $\partial_z\delta\mathbf{n}$ vanish, the compression term and the bend term drop out from the elastic free energy (2.2). The remaining terms involve only the radial and azimuthal components of the distortion fields. Moreover, there is no term that mixes different components. Observe that the topological condition (3.4) fixes the azimuthal component of $\mathbf{v}$. Among all configurations of the distortion fields with fixed azimuthal components, the configuration with $v_\rho=0$, $\delta n_\rho=0$ has the lowest energy. This means that the distortion fields induced by a single screw dislocation are not only cylindrically symmetric, but

also have a single azimuthal component. A vector field of such structure is solenoidal, and we can conclude that

$$\nabla \cdot \mathbf{v} = 0, \tag{3.7}$$

$$\nabla \cdot \delta\mathbf{n} = 0. \tag{3.8}$$

The last relation eliminates the splay contribution to the elastic free energy. Although Eqs. (3.6), (3.7), and (3.8) are obtained for a single screw dislocation, the superposition procedure guarantees that they remain valid even for the distortion fields produced by arbitrary systems of screw dislocations as long as the harmonic approximation is applicable.

A simple argument shows that Eq. (3.7) cannot hold in the presence of edge dislocations. Consider a single edge dislocation oriented in the y direction. As in the case of a screw dislocation, the translational symmetry of the distortion fields in the core direction together with the topological condition (3.4) makes the **v**-field orthogonal to the core direction, so $v_y = 0$. Then $\nabla \cdot \mathbf{v}$ reduces to $\partial_x v_x + \partial_z v_z$. It is easy to check that $\partial_x v_x$ and $\partial_z v_z$ have the same sign everywhere, so $\nabla \cdot \mathbf{v}$ never vanishes. The presence of additional edge dislocations does not modify this conclusion.

Thus we see that in the harmonic approximation, the constraint (3.7) provides a very clear distinction between systems of pure screw dislocations and other dislocation systems. Note that Eqs. (3.6) and (3.7) imply that smectic layers in the presence of screw dislocations are minimal surfaces, which are defined as surfaces of zero mean curvature. If **N** is a field of unit normals to a family of surfaces $\phi(x,y,z) = \text{const}$ filling the space, then the mean curvature of the surfaces in the family is proportional to $\nabla \cdot \mathbf{N}$ [18], the multiplicative constant chosen by convention. The field of unit normals to the smectic layers is

$$\mathbf{N} = \frac{\nabla\phi}{|\nabla\phi|} = \frac{\hat{z} + \mathbf{v}}{\sqrt{1 + 2v_z + \mathbf{v}^2}}. \tag{3.9}$$

Since v_z vanishes, $|\nabla\phi| = 1 + O(\mathbf{v}^2)$. So in the harmonic approximation the denominator is unity, and

$$\nabla \cdot \mathbf{N} = \nabla \cdot \mathbf{v} = 0. \tag{3.10}$$

B. Elastic energy of screw dislocations

Following [2], we can obtain an explicit solution for the distortion fields induced by a single screw dislocation. The **v** field is determined by equations (3.4) and (3.7) with $\mathbf{b}(\mathbf{x})$ given by Eq. (3.5). At infinity the smectic layers are undistorted, so $\mathbf{v} \to 0$ as $\rho \to \infty$. To emphasize that the problem is in fact two-dimensional, we rewrite Eqs. (3.4) and (3.7) as

$$\nabla_\perp \times \mathbf{v} = \mathbf{b}(\mathbf{x}), \tag{3.11}$$

$$\nabla_\perp \cdot \mathbf{v} = 0. \tag{3.12}$$

For our purposes, it is convenient to solve these equations in Fourier space. A general solution to Eq. (3.11) can be decomposed into longitudinal and transverse components with respect to the direction of $\mathbf{q}_\perp$. Equation (3.12) eliminates the longitudinal component, so we have

$$\mathbf{v}(\mathbf{q}_\perp) = i\frac{\mathbf{q}_\perp \times \mathbf{b}(\mathbf{q}_\perp)}{\mathbf{q}_\perp^2}, \tag{3.13}$$

where in the case of a single screw dislocation $\mathbf{b}(\mathbf{q}) = \hat{z}d\,\delta(q_z)$. The nematic director tilt field $\delta\mathbf{n}$ can be obtained from the Euler-Lagrange equations derived from the elastic free energy (2.2). Earlier we discovered that the compression, bend, and splay terms drop out. Then the elastic free energy reduces to

$$F = \frac{1}{2}\int d^3x [D(\nabla_\perp u + \delta\mathbf{n})^2 + K_2(\nabla_\perp \times \delta\mathbf{n})^2]$$

$$= \frac{1}{2}\int \frac{d^3q}{(2\pi)^2}[D|\mathbf{v}(\mathbf{q}_\perp) - \delta\mathbf{n}(\mathbf{q}_\perp)|^2 + K_2|\mathbf{q}_\perp \times \delta\mathbf{n}(\mathbf{q}_\perp)|^2]. \tag{3.14}$$

Variation of Eq. (3.14) with respect to u and $\delta\mathbf{n}$ leads to the following Euler-Lagrange equations:

$$\nabla_\perp \cdot (\mathbf{v} - \delta\mathbf{n}) = 0, \tag{3.15}$$

$$\nabla_\perp^2 \delta\mathbf{n} = \frac{1}{\lambda^2}(\delta\mathbf{n} - \mathbf{v}), \tag{3.16}$$

where $\lambda \equiv \lambda_2 = (K_2/D)^{1/2}$ is the twist penetration depth. The first equation is automatically satisfied. The solution of the second equation in Fourier space is

$$\delta\mathbf{n}(\mathbf{q}_\perp) = \frac{1/\lambda^2}{\mathbf{q}_\perp^2 + 1/\lambda^2}\mathbf{v}(\mathbf{q}_\perp). \tag{3.17}$$

In real space, the solutions for the distortion fields in polar coördinates ρ and ϕ are

$$\mathbf{v} = \frac{d}{2\pi\rho}\mathbf{e}_\phi, \tag{3.18}$$

$$\mathbf{v} - \delta\mathbf{n} = \frac{d}{2\pi\lambda}\mathcal{K}_1(\rho/\lambda)\mathbf{e}_\phi, \tag{3.19}$$

where $\mathcal{K}_1$ is the modified Bessel function of order 1. Substituting the distortion fields (3.13) and (3.17) into the elastic free energy (3.14), we find that the elastic energy cost per unit length of a single screw dislocation is

$$\frac{F_{\text{el}}^{(1)}}{L} = \frac{1}{2}Dd^2\int \frac{d^2q}{(2\pi)^2}\frac{1}{\mathbf{q}_\perp^2 + 1/\lambda^2}. \tag{3.20}$$

Since the smectic order exists only outside the dislocation core, the integration region has to be restricted to the disk $|\mathbf{q}_\perp| < 1/a$, where a is the core radius. Then the integral gives

$$\frac{F_{\rm el}^{(1)}}{L}=\frac{Dd^2}{8\pi}\ln\left(\frac{\lambda^2}{a^2}+1\right). \tag{3.21}$$

Note that in the extreme type I systems $\lambda\to 0$, so there is no elastic contribution to the screw dislocation energy in the harmonic approximation [4,17].

It is straightforward to generalize Eq. (3.20) to an arbitrary density of screw dislocations parallel to the z axis:

$$\frac{F_{\rm el}}{L}=\tfrac{1}{2}D\int\frac{d^2q}{(2\pi)^2}\frac{1}{\mathbf{q}_\perp^2+1/\lambda^2}|\overline{b}(\mathbf{q}_\perp)|^2, \tag{3.22}$$

where the scalar areal dislocation density $\overline{b}(\mathbf{q}_\perp)$ is defined via $\mathbf{b}(\mathbf{q})\equiv\hat{z}\overline{b}(\mathbf{q}_\perp)\delta(q_z)=\hat{z}d\,\delta(q_z)\Sigma_\alpha\exp\{iq_xx_\alpha\}\exp\{iq_yy_\alpha\}$.

IV. INTERACTION OF TWIST GRAIN BOUNDARIES

A twist grain boundary separates two smectic domains with layer normals that, while pointing in different directions, remain perpendicular to some axis. Physically, it can be implemented as an array of equidistant parallel screw dislocations. In this case topology imposes a constraint on the layer rotation angle $\Delta\Theta$. Rewriting the topological condition (3.1) in terms of the layer normal and the local layer spacing $d(\mathbf{x})$ [4],

$$\oint\frac{\mathbf{N}}{d(\mathbf{x})}\cdot d\mathbf{l}=n. \tag{4.1}$$

If we consider a rectangular integration path in the xy plane that surrounds one $n=1$ defect then, with d fixed, we find that

$$\frac{l_d}{d}[\,\delta\mathbf{N}_+-\delta\mathbf{N}_-\,]=1, \tag{4.2}$$

where $\delta\mathbf{N}$ is the projection of $\mathbf{N}$ onto the xy plane, d is the equilibrium layer spacing and l_d is the dislocation spacing. This change corresponds to the rotation of smectic layers by $\Delta\Theta=2\sin^{-1}(d/2l_d)$, which becomes d/l_d in the low-angle limit. It should be emphasized that although the rotation angle of the smectic layers is dictated by topology, topology in no way requires a specific orientation of defects in the grain boundary with respect to the smectic layers at infinity. Rather, this orientation is determined energetically. Leaving a detailed comparison of energetics of various dislocation systems outside the scope of this paper, here we will assume that pure screw dislocation systems are energetically preferable to systems of screw-edge dislocations with similar geometry and consider only those configurations of defects and smectic layers that correspond to pure screw dislocation systems. The formalism developed in the preceding section applies specifically to this kind of system.

The above result regarding the rotation angle of the smectic layers can be also obtained by considering the distortion fields. If the plane of the boundary is the yz plane and the dislocations are parallel to the z axis, then the dislocation source has the following form:

$$\mathbf{b}_{\rm tgb}(x,y,z)=\hat{z}d\,\delta(x)\sum_{n=-\infty}^{\infty}\delta(y-nl_d), \tag{4.3}$$

where l_d is the spacing between defects along the y axis. The layer tilt $\mathbf{v}$ induced by the source (4.3) can be obtained by superimposing the contributions of individual dislocations (3.18):

$$v_x(x,y)=\frac{d}{2\pi}\sum_{n=-\infty}^{\infty}\frac{y-nl_d}{x^2+(y-nl_d)^2}, \tag{4.4}$$

$$v_y(x,y)=-\frac{d}{2\pi}\sum_{n=-\infty}^{\infty}\frac{x}{x^2+(y-nl_d)^2}. \tag{4.5}$$

The sums can be computed explicitly with the help of the Poisson summation formula [19]:

$$v_x=\frac{d}{2l_d}\frac{\sin 2\pi y/l_d}{\cosh 2\pi x/l_d-\cos 2\pi y/l_d}, \tag{4.6}$$

$$v_y=-\frac{d}{2l_d}\frac{\sinh 2\pi x/l_d}{\cosh 2\pi x/l_d-\cos 2\pi y/l_d}. \tag{4.7}$$

The limiting form of v_x and v_y for large $|x|$ is

$$\mathbf{v}(x\to\pm\infty)=\pm\frac{d}{2l_d}\hat{y}, \tag{4.8}$$

which shows that the smectic layers undergo a rotation by d/l_d about the x axis as they cross the dislocation array at $x=0$. While the director relaxes to the layer normal in a distance of the order of the twist penetration depth λ, we see that the smectic layers relax to the undistorted asymptotic configuration within a distance l_d of the grain boundary.

The intensive energetic characteristic of a twist grain boundary is the elastic energy per unit area. It can be computed by the following limiting procedure. Instead of an infinite dislocation array (4.3), consider an array of N screw dislocations. The array extension in the y direction is Nl_d. Its elastic energy $F_{\rm el}(N)$ is given by Eq. (3.22). Then the elastic energy per unit interval of the y axis of a complete twist grain boundary can be taken as a limit of the ratio of the energy of a finite array to its extension in the y direction:

$$\frac{F_{\rm tgb}^{(1)}}{l_d}=\lim_{N\to\infty}\frac{F_{\rm el}(N)}{Nl_d}. \tag{4.9}$$

To implement this limit, we should consider the square of the amplitude of the areal dislocation density

$$|\overline{b}|^2=d^2\sum_{n=1}^{N}\sum_{n'=1}^{N}\exp[\,iq_yl_d(n-n')\,]. \tag{4.10}$$

As $N\to\infty$, note that $|\overline{b}|^2/N\to\Sigma_{n=-\infty}^{\infty}\exp\{iq_yl_dn\}$ and thus the energy per unit area of a twist grain boundary is

$$\frac{F_{\rm tgb}^{(1)}}{A}=\frac{Dd^2}{2l_d}\sum_{n=-\infty}^{\infty}\int\frac{d^2q}{(2\pi)^2}\frac{e^{iq_y l_d n}}{\mathbf{q}_\perp^2+1/\lambda^2}. \tag{4.11}$$

Note that $F_{\rm tgb}/A$ may be broken into an extensive part and the interaction part. This corresponds to a separation of the $n=0$ term from the rest of the sum:

$$\frac{F_{\rm tgb}^{(1)}}{A}=\frac{1}{l_d}\frac{F_{\rm el}^{(1)}}{L}+\frac{F_{\rm tgb}^{\rm int}(1)}{A}. \tag{4.12}$$

The interaction part $F_{\rm tgb}^{\rm int}$ can be written as a sum over contributions of dislocation pairs at distances $l_d, 2l_d, \ldots$:

$$\begin{aligned}\frac{F_{\rm tgb}^{\rm int}(1)}{A}&=\frac{Dd^2}{2l_d}\sum_{\substack{n=-\infty\\ n\neq 0}}^{\infty}\int\frac{d^2q}{(2\pi)^2}\frac{e^{iq_y l_d n}}{\mathbf{q}_\perp^2+1/\lambda^2}\\ &=\frac{Dd^2}{2l_d}\sum_{n=1}^{\infty}\int_{-\infty}^{\infty}\frac{dq_y}{2\pi}\frac{\cos q_y l_d n}{\sqrt{q_y^2+1/\lambda^2}}\\ &=\frac{Dd^2}{2\pi l_d}\sum_{n=1}^{\infty}\mathcal{K}_0\left(\frac{l_d n}{\lambda}\right),\end{aligned} \tag{4.13}$$

where $\mathcal{K}_0$ is the modified Bessel function of order zero. As expected, this result closely resembles the interaction energy of parallel vortices in the London limit [20,21]:

$$\frac{F_{\rm Abr}^{\rm int}}{A}=\frac{1}{n_L}\frac{\Phi_0^2}{8\pi^2\lambda^2}\sum_i\sum_{j>i}\mathcal{K}_0\left(\frac{r_{ij}}{\lambda}\right), \tag{4.14}$$

where $\Phi_0=2\pi\hbar c/e^*$ is a quantum of the magnetic flux, n_L is the vortex areal density, and λ is the magnetic field penetration depth.

Our next goal is to compute the interaction energy of twist grain boundaries. Before we consider the grain boundary system in the TGB$_A$ phase, let us limit our consideration to systems of finite number of parallel low-angle grain boundaries that are sufficiently separated so that the harmonic approximation (2.2) is applicable. Again, topology completely determines the relative orientations of the smectic layers in different smectic blocks. To ensure that the defects are pure screw dislocations, we require that the defects in adjacent grain boundaries be rotated by $\Delta\Theta=d/l_d$ and, in addition, that the outermost smectic blocks be rotated by the same angle, but in the opposite directions with respect to the defects in the middle of the system. In comparison with the calculation for a single grain boundary, we are dealing now with more general defect systems where not all defects are parallel to each other. Our formalism easily handles this situation.

Consider a system that contains only two twist grain boundaries separated by a distance l from each other. The angle between directions of the dislocation lines in these two boundaries is $\theta=\Delta\Theta=d/l_d$. We may implement this by taking one grain boundary at $x=-l/2$, rotated by $-\theta/2$ and the other boundary at $x=l/2$, rotated by $\theta/2$ where $\theta=d/l_d$. The dislocation density for this complexion is the sum of the contributions from the two grain boundaries, $\mathbf{b}=\mathbf{b}_{\rm tgb}^{(1)}+\mathbf{b}_{\rm tgb}^{(2)}$, where

$$\begin{aligned}\mathbf{b}_{\rm tgb}^{(1)}(q_x,q_y,q_z)&=[\hat{z}-(\theta/2)\hat{y}]2\pi d e^{-iq_x l/2}\delta[q_z-(\theta/2)q_y]\\ &\times\sum_{n=-\infty}^{\infty}\exp[i(q_y+\theta q_z/2)nl_d],\end{aligned} \tag{4.15}$$

$$\begin{aligned}\mathbf{b}_{\rm tgb}^{(2)}(q_x,q_y,q_z)&=[\hat{z}+(\theta/2)\hat{y}]2\pi d e^{iq_x l/2}\delta[q_z+(\theta/2)q_y]\\ &\times\sum_{n=-\infty}^{\infty}\exp[i(q_y-\theta q_z/2)nl_d].\end{aligned} \tag{4.16}$$

We may transform the sums in the above expression into a sum of delta functions via the Poisson summation formula:

$$\begin{aligned}&\mathbf{b}_{\rm tgb}^{(1)}(q_x,q_y,q_z)\\ &=[\hat{z}-(\theta/2)\hat{y}]\delta[q_z-(\theta/2)q_y]\frac{2\pi d}{l_d}e^{-iq_x l/2}\\ &\times\sum_{m=-\infty}^{\infty}\delta\left[q_y+\theta q_z/2-\frac{2\pi m}{l_d}\right],\end{aligned} \tag{4.17}$$

$$\begin{aligned}&\mathbf{b}_{\rm tgb}^{(2)}(q_x,q_y,q_z)\\ &=[\hat{z}+(\theta/2)\hat{y}]\delta[q_z+(\theta/2)q_y]\frac{2\pi d}{l_d}e^{iq_x l/2}\\ &\times\sum_{m=-\infty}^{\infty}\delta\left[q_y-\theta q_z/2-\frac{2\pi m}{l_d}\right].\end{aligned} \tag{4.18}$$

By virtue of linear superposition, the energy of this dislocation density will be the sum of three terms. Two of these terms are simply the self-energies of the two individual grain boundaries that we have calculated above. The interaction energy comes from the cross term that is of the form:

$$F_{\rm tgb}^{\rm int}(2,l)=2\int\frac{d^3q}{(2\pi)^3}b_{\rm tgb}^{(1),i}(\mathbf{q})M_{ij}(\mathbf{q})b_{\rm tgb}^{(2),j}(-\mathbf{q}), \tag{4.19}$$

where $M_{ij}(\mathbf{q})$ is the general interaction kernel that accounts for both screw and edge dislocations [2]. Upon inspection of Eqs. (4.17) and (4.18), we note that: (1) Since $(d/l_d)=\theta$ the $\hat{y}$ components of the dislocation densities may be ignored since we are only working to quadratic order in $\theta=\Delta\Theta$, and (2) in the product $b_{\rm tgb}^{(1)}b_{\rm tgb}^{(2)}$ only the $m=0$ terms in Eq. (4.17) contribute because of the delta-function constraints. As a result, only the $q_z=0$ and $q_y=0$ modes of $\mathbf{b}_{\rm tgb}^{(1)}$ and $\mathbf{b}_{\rm tgb}^{(2)}$ contribute. Moreover, since the $q_y=0$ modes of the layer normals in Eqs. (4.6) and (4.7) relax to their asymptotic values immediately, we see that we have constructed a globally consistent layer structure between the boundaries. Thus we may use Eq. (3.22) to evaluate the interaction energy:

$$\frac{F_{\mathrm{tgb}}^{\mathrm{int}}(2,l)}{A}=\frac{Dd^2}{2l_d}\frac{1}{l_d}\int_{-\infty}^{\infty}\frac{dq_x}{2\pi}\frac{e^{iq_xl}+e^{-iq_xl}}{q_x^2+1/\lambda^2}=\frac{Dd^2}{2l_d}\frac{\lambda}{l_d}e^{-l/\lambda}. \tag{4.20}$$

Note that since only the $q_y=0$ modes contribute, the interaction energy is independent of arbitrary phason shifts of the grain boundaries along y. In the harmonic approximation, the interaction energy of grain boundaries in a system of several twist grain boundaries breaks down into the sum of contributions of individual grain boundary pairs. Since the harmonic theory admits linear superposition, the result (4.20) can be applied to any angle of rotation at any separation l as long as the grain boundaries are composed purely of screw defects.

Another way to look at this result is to consider the behavior of the director between the grain boundaries. We may expand the director and displacement fields in Fourier modes at all the reciprocal lattice vectors **G**. In the harmonic approximation, director and displacement fields from different sources add linearly. Thus if no pairs of grain boundaries have dislocation axes parallel or antiparallel and dislocations in each boundary are straight, each distortion (displacement $u_{\mathbf{G}}$ or $\delta\mathbf{n}_{\mathbf{G}}$) for a given reciprocal lattice vector $\mathbf{G}\neq 0$ arises from a unique grain boundary. Thus finite reciprocal lattice vector distortions from different grain boundaries do not interact. Each grain boundary, however, produces a $\mathbf{G}=0$ director distortion $\delta\mathbf{n}_0$, which is sensitive to the presence of other grain boundaries. The origin of interactions between grain boundaries is thus $\delta\mathbf{n}_0$, and we can calculate these interactions by applying appropriate boundary condition to $\delta\mathbf{n}_0$. For an isolated grain boundary, $\delta\mathbf{n}_0=(0,\delta n_y,0)$ reaches constant asymptotic values of $(0,\pm\theta)$. If there is more than one grain boundary, $\delta\mathbf{n}_0$ has to rotate through the angles determined by the dislocation complexion in a shorter distance and at greater energy cost. Consider two walls with dislocation separation l_d located at $x=\pm l/2$. If we consider Eqs. (3.15) and (3.16) in this situation we see that $\boldsymbol{\nabla}_\perp\cdot\mathbf{v}=\boldsymbol{\nabla}_\perp\cdot\delta\mathbf{n}=0$ since both $\mathbf{v}$ and $\delta\mathbf{n}$ only have components along $\hat{y}$ but only depend on x. Thus Eq. (3.16) becomes:

$$\partial_x^2\delta n_y=\frac{1}{\lambda^2}[\delta n_y+\boldsymbol{\nabla}_\perp u]. \tag{4.21}$$

We have three regions to consider. For $x\leqslant -l/2$ we have

$$\boldsymbol{\nabla}_\perp u=\theta\hat{y}, \tag{4.22}$$

$$\delta n_y=-\theta+Ae^{(x+l/2)/\lambda}, \tag{4.23}$$

while between $x=-l/2$ and $x=l/2$

$$\boldsymbol{\nabla}_\perp u=0, \tag{4.24}$$

$$\delta n_y=B\frac{\sinh(x/\lambda)}{\sinh(l/2\lambda)}, \tag{4.25}$$

and for $x\geqslant l/2$

$$\boldsymbol{\nabla}_\perp u=-\theta\hat{y}, \tag{4.26}$$

$$\delta n_y=\theta-Ce^{-(x-l/2)/\lambda}. \tag{4.27}$$

Continuity of the director forces $C=A=\theta-B$. Inserting these solutions into into the energy (3.14) we have

$$\frac{F(l)}{A}=D\lambda[(B-\theta)^2+B^2\coth(l/2\lambda)]. \tag{4.28}$$

Minimizing over the free parameter B and using $\theta=d/l_d$, we find

$$\frac{F(l)}{A}=\frac{D\lambda d^2}{l_d^2}\frac{\coth(l/2\lambda)}{1+\coth(l/2\lambda)}=\frac{D\lambda d^2}{2l_d^2}[1+e^{-l/\lambda}]. \tag{4.29}$$

The energy of interaction is simply

$$\frac{\Delta F}{A}=\frac{F(l)-F(\infty)}{A}=\frac{Dd^2}{2l_d^2}\lambda e^{-l/\lambda}, \tag{4.30}$$

which agrees with our previous result (4.20). This shows that the energy of interaction comes from the ''confinement'' of the director—it is forced to twist from $-\theta/2$ to $\theta/2$ in a length on the order of a few l.

V. TGB$_A$ PHASE

In the preceding section we showed that in a system composed of finite number of low-angle twist grain boundaries the energy of the dislocation interaction within a grain boundary and the energy of the interboundary interaction decay exponentially with distance. It suggests that the dislocation arrangement in the TGB$_A$ phase could be treated as well within the same computational framework, even though the angles between the directions of dislocations in the entire system are not restricted to be small. Indeed, when the grain boundaries are low angle, the dislocations that cannot be described as nearly parallel are separated by the distance of many grain sizes l_b. It is reasonable to hope that we can find a regime where l_b is sufficiently large so that the interaction part of the TGB$_A$ elastic free energy density is dominated by the interaction of the dislocations in a few nearby grain boundaries. In this case our formalism would be reliable.

Provided that that we are in the correct regime, the preceding section supplies us with all the essential ingredients to compute the interaction energy of dislocations arranged in the TGB$_A$ structure (Fig. 1). To construct an appropriate dislocation source, we need to combine the sources for individual twist grain boundaries at positions 0, $\pm l_b$, $\pm 2l_b$, ... along the pitch axis. The grain boundaries at different positions are distinguished by the direction of defects and, in addition, might be arbitrarily shifted in the direction perpendicular to the pitch axis. We may, through superposition, use the results from the last section to find

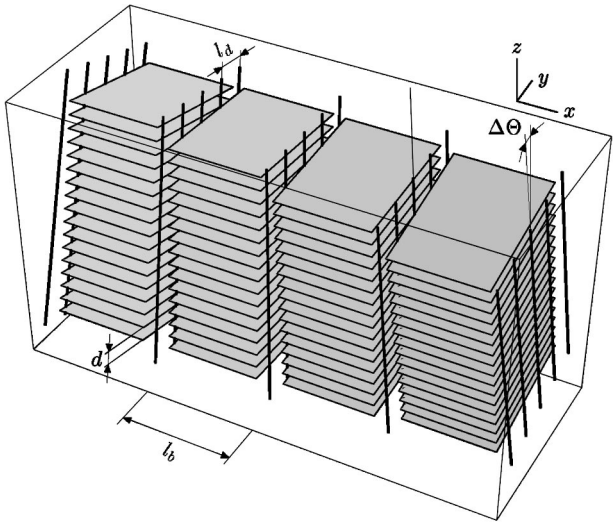

FIG. 1. Schematic representation of the TGB_A phase.

$$f_{\mathrm{TGB}}^{\mathrm{int}}=\frac{Dd^2}{2l_b l_d}\left[\frac{1}{\pi}\sum_{n=1}^{\infty}\mathcal{K}_0\left(\frac{l_d n}{\lambda}\right)+\frac{\lambda}{l_d}\sum_{n=1}^{\infty}e^{-l_b n/\lambda}\right]. \quad (5.1)$$

We can understand the interaction term by again considering the confinement energy of the director. In the case of the full TGB_A structure, each ''cell'' between the grain boundaries must be identical. Thus we may use Eq. (4.24) with $B=\theta/2$ to calculate the energy for each cell. We find complete agreement with the interaction term above.

In addition to the elastic energy of interacting screw dislocations, the total free energy of the TGB_A structure includes two extensive terms that depend only on the dislocation density $1/(l_b l_d)$ and not on the details of a particular dislocation arrangement. These terms are the extensive part of the screw dislocation energy density and the chiral energy term:

$$f_{\mathrm{tot}}=f_{\mathrm{TGB}}^{\mathrm{int}}+f_{\mathrm{disl}}+f_{\mathrm{ch}} \quad (5.2)$$

$$=\frac{Dd^2}{2l_b l_d}\left[\frac{1}{\pi}\sum_{n=1}^{\infty}\mathcal{K}_0\left(\frac{l_d n}{\lambda}\right)+\frac{\lambda}{l_d}\sum_{n=1}^{\infty}e^{-l_b n/\lambda}\right]+\frac{E}{l_b l_d}-\frac{hd}{l_b l_d}, \quad (5.3)$$

where E is the energy cost per unit line of an individual screw dislocation. In the free energy density (5.2), the total energy cost of dislocations given by the first two terms competes with the gain in the chiral energy. The twist penetration depth λ sets the length scale for l_d and l_b. Inspecting Eq. (5.2), we see that the optimal values of l_d/λ, l_b/λ are controlled by a single combination of the material parameters

$$\alpha=\frac{2(hd-E)}{Dd^2}. \quad (5.4)$$

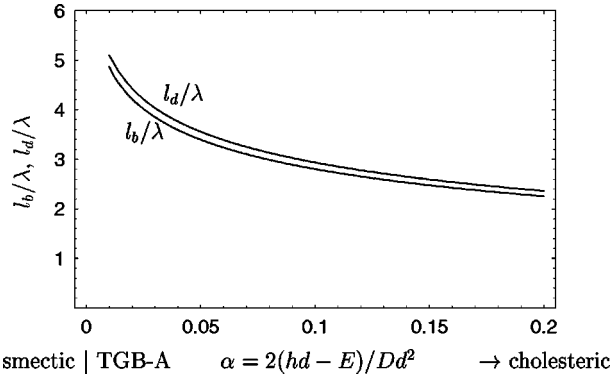

FIG. 2. Dependence of the dislocation spacing within a grain boundary l_d and the grain size l_b on the control parameter $\alpha=2(hd-E)/Dd^2$. At some large value of α there is a transition to the cholesteric phase (at h_{C2}) while $\alpha=0$ corresponds to the smectic-TGB_A transition.

We minimized of the energy density (5.2) with respect to l_d/λ and l_d/λ numerically. The results are presented in Fig. 2. We can make several observations regarding our results. As is directly evident from Fig. 2, there is a range of α where the preferred values of l_d and l_b are of several λ and, moreover, the ratio l_d/l_b is close to 1. According to the remarks at the beginning of this section, this kind of geometry validates our computational techniques. To see how much far-away grain boundaries contribute to the establishment of the dislocation lattice structure, we computed the positions of minima for free energy densities obtained from Eq. (5.2) by truncating the sums over n to one, two, and three terms. The results of this computation are presented in Fig. 3, which demonstrate that in the range $0<\alpha<0.2$, which corresponds to $l_b, l_d > 2.5\lambda$, the lattice structure is determined almost entirely by the interactions of nearest and next-to-nearest twist grain boundaries.

A very interesting result emerges regarding the ratio of the lattice parameters l_b/l_d. It turns out that the ratio is

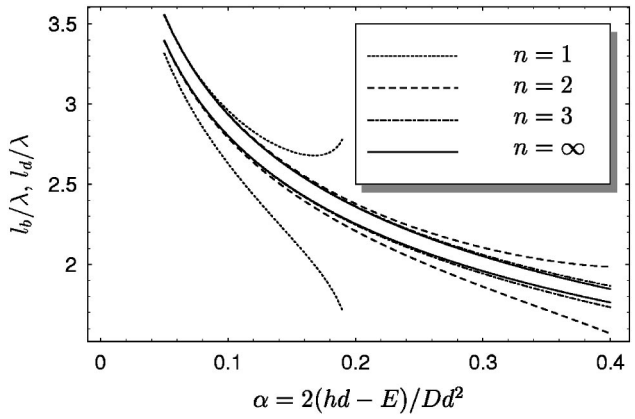

FIG. 3. Dependence of the minima positions on the number of terms kept in the sum over grain boundaries in the free energy density (5.2). The style of each curve reflects the number of terms used in its computation. The upper set of curves correspond to l_d/λ, while the lower curves correspond to l_b/λ. The solid curves are the same curves as in Fig. 2.

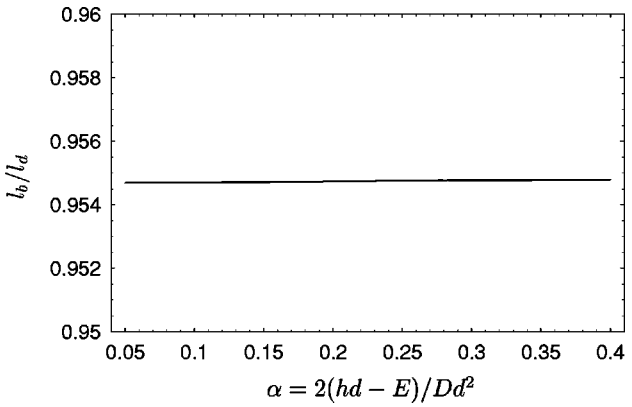

FIG. 4. Dependence of l_b/l_d on the control parameter α. Note that it is nearly independent of α.

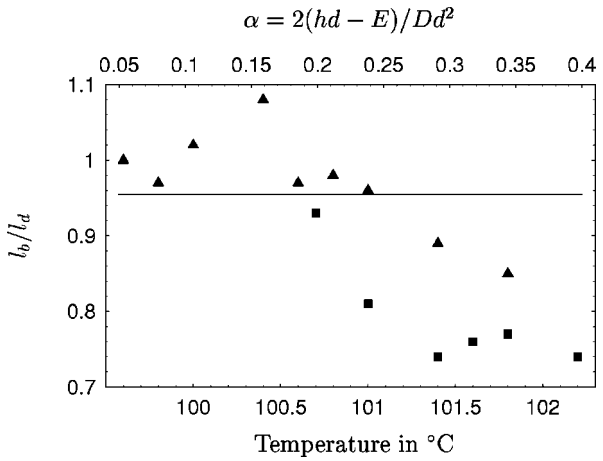

FIG. 5. Experimental dependence of l_b/l_d on temperature. The data set marked with triangles is taken from [15], the data set marked with boxes was provided courtesy of Navailles. The first set of data was taken while increasing temperature, while the latter was taken in a run with decreasing temperature. Note that the grain rotation angle increases from 6° for the lowest temperature to 9° for the highest temperature.

nearly constant for a very wide range of values of the control parameter α (Fig. 4). This prediction should be compared to the experimental values of l_b/l_d measured by Navailles and co-workers [15].

VI. CONCLUSIONS

The theory of the screw dislocation interaction in the TGB_A phase in the low-angle grain boundary limit was constructed by analogy with the theory of vortex interaction in the Abrikosov phase in the high-κ limit. The resulting theory was applied to the calculation of the lattice parameters of the screw dislocation arrangement. We found that in this limit the ratio of the two lattice parameters l_b/l_d remains pratically constant over a very wide range of the control parameter. The value of the ratio is 0.95. It is interesting to note this value is within several thousands of the value obtained by Renn and Lubensky [1] in the opposite limit $h \to h_{c2}$ for a specific value $K/K_2 = 0$. Whether this is accidental or not remains to be discovered. In contrast to the Renn and Lubensky result, the value of l_d/l_b obtained here is independent of K_1 and K_3. This value is consistent with the experimental data of Navailles and co-workers [15] (Fig. 5).

Recent work [19] that studied the nonlinear elasticity of smectic liquid crystals showed that defects in the same grain boundary had power-law interactions. One might expect, in general, that the interaction between grain boundaries would remain exponential. It would seem then that the grain boundaries would move closer together as the defects in the boundaries would move further apart, casting some doubt on our result (and on experiment). In the absence of director modes, the nonlinear elasticity is [19]

$$F = \tfrac{1}{2} \int d^3x \{ B[\partial_z u - \tfrac{1}{2}(\nabla u)^2]^2 + K(\nabla_\perp^2 u)^2 \}. \quad (6.1)$$

In this nonlinear theory the director and the layer normal are locked together so that $\mathbf{n} = -\nabla\phi/|\nabla\phi|$. While a full analysis of the energetics of two interacting grain boundaries will be the focus of further work, we can, in the spirit of the analysis at the end of Sec. IV, consider a single, distorted screw dislocation:

$$u(x,y) = \tan^{-1}\left[\frac{\pi y}{l \tan(\pi x/l)} \right]. \quad (6.2)$$

The layer normal of this dislocation relaxes in the usual way along the y direction but relaxes to its asymptotic value in the confined region between $x = \pm l/2$. It is straightforward to calculate the nonlinear energy of this defect and to find the ''confinement'' energy by subtracting the $l = \infty$ value. Expanding in powers of l^{-1} we have

$$\nabla_\perp^2 u \approx \frac{\pi^2}{l^2} \frac{2xy(x^2 - y^2)}{(x^2 + y^2)^2}, \quad (6.3)$$

$$(\nabla u)^2 \approx \frac{1}{x^2 + y^2} + \frac{\pi^2}{l^2} \frac{2x^2y^2 - \frac{2}{3}x^4}{(x^2 + y^2)^2}. \quad (6.4)$$

It is clear that the l dependence of the confinement energy scales as l^{-2} that can balance the l_d^{-2} interaction found between defects in the same grain boundary [19]. We shall explore this further in future work.

ACKNOWLEDGMENTS

It is a pleasure to acknowledge fruitful conversations with L. Navailles, B. Pansu, and R. Pindak. I.B. and R.D.K. were supported through NSF CAREER Grant No. DMR97-32963 and NSF Grant No. INT99-10017. R.D.K was supported, in addition, by the Alfred P. Sloan Foundation and a gift from L.J. Bernstein. T.C.L was supported through NSF Grant No. DMR97-30405.

[1] S. R. Renn and T. C. Lubensky, Phys. Rev. A **38**, 2132 (1988).
[2] P. M. Chaikin and T. C. Lubensky, *Principles of Condensed Matter Physics* (Cambridge University Press, Cambridge, 1995).
[3] P.-G. de Genness, Solid State Commun. **10**, 753 (1972).
[4] P.-G. de Gennes and J. Prost, *The Physics of Liquid Crystals*, 2nd ed. (Claredon Press, Oxford, 1993).
[5] A. B. Harris, R. D. Kamien, and T. C. Lubensky, Phys. Rev. Lett. **78**, 1476 (1997); **78**, 2867(E) (1997); Rev. Mod. Phys. **71**, 1745 (1999).
[6] Z. Hao and J. R. Clem, Phys. Rev. B **46**, 5853 (1992).
[7] A. A. Abrikosov, Zh. Éksp. Teor. Fiz. **32**, 1442 (1957) [Sov. Phys. JETP **5**, 1174 (1957)].
[8] A. L. Fetter and P. C. Hohenberg, in *Superconductivity*, edited by R. D. Parks (Dekker, New York, 1969).
[9] E. H. Brandt, Rep. Prog. Phys. **58**, 1465 (1995).
[10] J. W. Goodby, M. A. Waugh, S. M. Stein, E. Chin, R. Pindak, and J. S. Patel, Nature (London) **337**, 449 (1989).
[11] J. W. Goodby, M. A. Waugh, S. M. Stein, E. Chin, R. Pindak, and J. S. Patel, J. Am. Chem. Soc. **111**, 8119 (1989).
[12] G. Srajer, R. Pindak, M. A. Waugh, J. W. Goodby, and J. S. Patel, Phys. Rev. Lett. **64**, 1545 (1990).
[13] K. J. Ihn, J. A. N. Zasadzinski, R. Pindak, A. J. Stanley, and J. Goodby, Science **258**, 275 (1992).
[14] H. T. Nguyen, A. Bouchta, L. Navailles, P. Barois, N. Isaert, R. J. Twieg, A. Maaroufi, and C. Destrade, J. Phys. II **2**, 1889 (1992).
[15] L. Navailles, B. Pansu, L. Gorre-Talini, and H. T. Nguyen, Phys. Rev. Lett. **81**, 4168 (1998).
[16] N. Isaert, L. Navailles, P. Barois, and H. T. Nguyen, J. Phys. II **4**, 1501 (1994).
[17] M. Kléman, *Points, Lines, and Walls: in Liquid Crystals, Magnetic Systems, and Various Magnetic Media* (Wiley, New York, 1983).
[18] T. Frankel, *The Geometry of Physics* (Cambridge University Press, Cambridge, 1997).
[19] R. D. Kamien and T. C. Lubensky, Phys. Rev. Lett. **82**, 2892 (1999).
[20] P.-G. de Gennes, *Superconductivity of Metals and Alloys* (W. A. Benjamin, New York, 1966).
[21] M. Tinkham, *Introduction to Superconductivity*, 2nd ed. (McGraw-Hill, New York, 1996).